

Nanostructured SiC as a promising material for the cold electron emitters

A.M. Goriachko¹, M.V. Strikha^{1,2}

¹Taras Shevchenko National University of Kyiv, Faculty of Radiophysics, Electronics and Computer Systems, 4g, prospect Akademika Hlushkova, 03022 Kyiv, Ukraine

²V. Lashkaryov Institute of Semiconductor Physics, National Academy of Sciences of Ukraine, 41, prospect Nauky, 03680 Kyiv, Ukraine
E-mail: maksym.strikha@gmail.com

Abstract. In this paper, the novel cold electron emitters based on nanostructured SiC layers covering the Si(001) substrate have been proposed. Their main advantage is an extremely simple and cost-effective manufacturing process based on the standard microelectronics-grade silicon wafers with no ultra-high vacuum required and no complicated chemical deposition processes or toxic chemicals involved. It integrates within a single technological step both the SiC growth and nanostructuring the surface in the form of nanosized protrusions, which is extremely beneficial for cathode applications. A simple mathematical model predicts field emission current densities and turn-on electric fields, which would allow practical device applications. According to our estimations, emission currents in the milli-Amp range can be harvested from one square centimeter of the cathode surface with electric field close to 10^7 V/m. So, the nanostructured SiC can be the promising material for the cold electron emitters.

Keywords: cold electron emitters, nanostructured SiC layers, current density.

<https://doi.org/10.15407/spqeo24.04.355>

PACS 79.70.+q, 81.07.-b, 81.16.-c, 81.40.-z, 85.45.Db

Manuscript received 28.05.21; revised version received 29.06.21; accepted for publication 10.11.21; published online 23.11.21.

1. Introduction

Intensive study of the novel electron sources for field emission (FE) devices, based on wide gap materials like GaN, diamond *etc.*, is being carried out in recent years (see, *e.g.* [1] and Refs. therein). The unique SiC properties (see, *e.g.* [2]), its high chemical and thermal stability makes this semiconductor promising for numerous applications. Namely, wide band gap (3.03 eV for 6H-SiC and 4H-SiC) permits SiC devices to operate at rather high temperatures without suffering from intrinsic conduction effects. Extremely high breakdown electric field (2.4×10^4 MV/m) enables SiC to withstand a voltage gradient over eight times greater than for Si or GaAs without undergoing an avalanche breakdown. At room temperature, SiC has a higher thermal conductivity than any metal. This property enables SiC devices to operate at extremely high power levels and still dissipate large amounts of excess heat. High saturated electron drift velocity in SiC (2×10^5 m/s for $F > 2 \times 10^7$ V/m) permits a high frequency operation. These unique properties can make SiC suitable for applications in vacuum electronics as well.

In this paper, we study nanostructured SiC layers on the Si(001) substrate as a promising novel material for the cold FE. The effective FE device operation needs availability of three factors: existence of a sufficient reservoir of electrons; good channel of electron supply to the emitting surface; high emitting properties of this surface. The energy band diagram of the proposed structure is presented in Fig. 1. A highly doped n^+ -type Si substrate can serve as the electrons reservoir. The nanostructured layer of SiC with electron conductivity (the latter can be achieved by doping of different SiC modifications with N. See, *e.g.* [3, 4]) can be grown on top of this substrate. To enhance emission from the SiC surface, it is helpful to shape it in the form of an array of protrusions with small radii of curvature. In this case, an electric field on the protrusions' apexes will be amplified in comparison to the value corresponding to the geometrically flat surface (provided all other conditions unchanged), serving as a cathode to which a negative potential is applied relatively to the ground. A stronger electric field will effectively reduce the height and thickness of the FE tunneling barrier, thus leading to higher electron emission current.

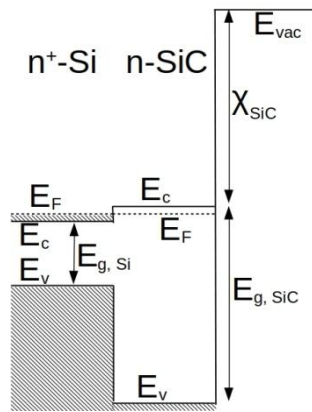


Fig. 1. Film/substrate system under examination: n^+ -Si substrate as an electron reservoir, wide-gap SiC as an emitter for FE. Hatching depicts the filled electron states.

2. Manufacturing process and characterization

In this section, we consider possible technological routes to practical realization of the theoretical concept described above. A straightforward way is to grow a SiC layer of sufficient thickness on the top of Si substrate by means of a suitable chemical vapor deposition (CVD) process, then use optical or electron beam nanolithography technique in order to achieve a desired morphology of the SiC layer. This route, although capable of producing a strictly pre-defined geometry of the nano-protrusions as well as their relative placement, has a substantial drawback of high cost and complexity. Namely, in addition to the SiC growth step it requires such additional steps as deposition, exposure and dissolution of the resist layer, etching of the SiC layer, rinsing, *etc.* Alternatively, one can try to develop a self-assembly process, with SiC growth and nanoprotusions formation combined into a single step. Potentially, it can reduce the cost of manufacturing the FE devices by a rather substantial margin.

When it comes to creating nanostructures on the initially flat surface, which serves as one of capacitor's electrodes, a strategy proposed by V. Gill *et al.* [5] seems to be extremely promising. They conclude that minimization of the system's free energy can lead to self-assembly of micro- to nano-scale islands on the conducting surface, provided a self-diffusion of its constituent material is activated. It is then a matter of tuning the value of surface diffusion coefficient (in practice this can be performed by changing the substrate's temperature), the capacitor's geometry and the voltage applied to it in order to achieve the desired surface morphology. As a source of carbon for SiC deposition, a number of pyrolytically decomposing hydrocarbon molecules can be taken. For example, a model hydrocarbon precursor C_2H_2 was shown to produce SiC, if admitted to the Si(001) surface at temperatures between 1000 and 1200 °C [6]. C_2H_2 is not unique in this role, and as demonstrated recently by one of us [7], even an uncontrolled residual atmosphere

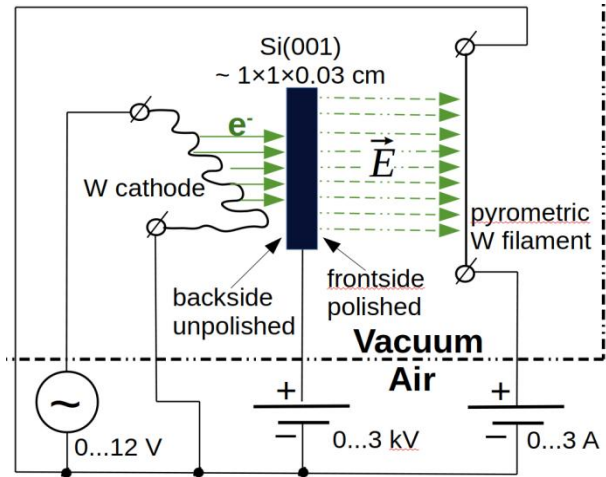


Fig. 2. Experimental setup for nanostructures self-assembly driven by an electric field. The cathode, sample and pyrometric filament are mounted in an ultra-high vacuum chamber. Voltages and currents are delivered from outside of the chamber by means of metal-ceramic electrical vacuum feedthroughs. The sample and pyrometric filament can be observed from the outside of the chamber through the vacuum viewport.

of the typical vacuum chamber, which is known to contain various hydrocarbon molecules, can deliver carbon to the semiconductor surface through a pyrolytic decomposition.

Our experimental setup, which was used for SiC nanostructured growth on the Si(001) substrate is shown in Fig. 2. It was constructed inside a standard stainless steel ultrahigh vacuum chamber, with a base pressure of 3×10^{-10} mbar achieved by oil-free pumping. We have used samples cut from microelectronics grade single side polished Si(001) wafers. The backside of the sample (unpolished side) was bombarded by electrons emitted from a compact thermionic cathode, which consisted of a tungsten wire directly heated by passing of alternative current from a regulated power supply. An accelerating DC voltage up to 3 kV was applied between the cathode and the sample, determining the electrons kinetic energy that is to be dissipated as heat inside the sample. Varying the accelerating voltage and the electron emission current from the cathode (by changing its temperature), we could achieve the same power dissipated in the sample at different values of the electric field at the front side (polished) surface. The counter electrode for creating this electric field was a 20 cm long W filament stretched 1 cm away and running parallel to the Si(001) surface. This filament was also used as a simple pyrometer by means of its visual observation through an appropriate vacuum viewport. As long as the wire was not discernible on the silicon surface background, their temperatures were estimated as equal. In its turn, the temperature of the pyrometric wire of the known diameter can be set precisely by selecting the value of the current flowing through it (adopting an approximation of infinite length).

After *in-situ* thermal treatment under the influence of electric field and cooling down to room temperature, the samples were investigated *ex-situ* by means of non-contact atomic force (AFM) microscopy in the ambient environment.

Initially, we prepared an atomically clean silicon surface by means of “outgassing” the silicon sample at 600 °C for several hours followed by repeated cycles of “flash”-annealing at 1200 °C (typically several dozen cycles). Each cycle’s duration was typically several dozens of seconds, limited by a strict requirement of keeping the residual gases pressure close to 10^{-10} mbar. The acceleration voltage for electron bombardment was equal to 1 kV. In Fig. 3a, we show an AFM image of the Si(001) surface prepared in accord to this procedure. The surface is mostly flat, except for some minor contamination by dust particles, which is unavoidable as long as the sample is in the ambient environment. A detailed *in-situ* investigation of this surface by means of scanning tunneling microscopy (STM), which was reported previously by one of us [8], has demonstrated that it consists of atomically flat terraces separated by single atomic steps, with a 2×1 dimer row reconstruction on top of each terrace. This fact proves beyond any doubt that the atomically clean Si(001) surface was indeed achieved by the preparation procedure described above.

Next, we used an identical preparation procedure in terms of the thermal treatment regiment, however the electron bombardment was performed with 2.6 keV accelerating voltage. The AFM image of this sample is shown in Fig. 3b. The only physically meaningful difference between the cases of Figs 3a and 3b is a higher electric field at the sample’s surface in the latter case. Obviously, it produces well protruding silicon nanocrystals on top of the flat background. This result is perfectly in-line with the prediction of V. Gill *et al.* [5]. In simple terms it can be explained in the following way: at 1200 °C there is a rapid self-diffusion within the surface layer of the sample. This leads to stochastic transport of silicon atoms, hence fluctuations in the form of local accumulations of sample’s material. They act as protrusions, decreasing the local radius of surface curvature and amplifying the electric field in these locations. As a result, in-plane surface gradients of electric field arise, and the atoms diffusing around the neighboring surface areas start to be dragged into the stronger electric field locations as induced electric dipoles. This leads to even greater accumulation of matter in such locations, and the process is self-amplifying through a positive feedback. Therefore, redistribution of mass takes place on the surface, resulting in growth of stochastically positioned protrusions, limited by field evaporation of atoms from their apexes. From Figs 3a and 3b, it is obvious that a minimal critical electric field on the nominally flat surface is required to initiate the self-assembly process.

The surface in Fig. 3b can serve as a substrate for the SiC layer growth in order to create the structure as shown in Fig. 1. If used as a field emitter, then a stronger electric field on the apexes of protrusions will enhance its

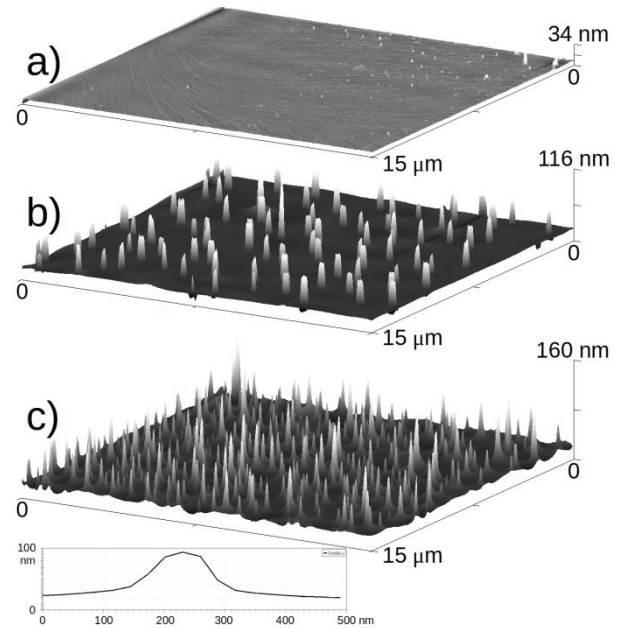


Fig. 3. Three-dimensional renderings of AFM images inherent to the Si(001) surface after vacuum annealing at 1200 °C in different conditions. All images are $15\times 15\ \mu\text{m}$ in lateral size and are drawn at the same vertical scale. a) Annealing with 1 kV accelerating voltage and base pressure of 3×10^{-10} mbar; b) 2.6 kV, 3×10^{-10} mbar; c) 2.6 kV, 3×10^{-8} mbar. The inset in (c) shows a cross-section of a typical nanoprotusion drawn with identical scales on the lateral and vertical axes.

emission properties. However, a clear technological disadvantage is the ultra-high vacuum requirement, making the manufacturing of such emitters more time consuming and expensive. In a stainless steel vacuum chamber, residual gas pressures in the ultra-high vacuum range can only be achieved after the so-called “baking”, which is essentially heating the entire chamber at several hundred degrees for dozens of hours. This is the most time-consuming step in the process of pumping down to 10^{-10} mbar range, which is absolutely necessary for obtaining an atomically clean silicon surface. However, it is extremely desirable to eliminate it, if a manufacturing process for practical applications is being developed. In this case, no “baking” is performed and the base pressure is in the 10^{-8} mbar range, the excess residual gases being rich of carbon.

Fig. 3c shows the AFM image of the Si(001) surface annealed in the same manner as in Fig. 3b (1200 °C, 2.6 kV) but in the “non-baked” conditions of the vacuum chamber with the base pressure of 3×10^{-8} mbar. As one can see, this procedure yields even better surface morphology with denser packing of sharper nanoprotusions than for 3×10^{-10} mbar. Being based on conclusions of [6, 7], it is reasonable to assume that there is a SiC layer on top of silicon at the sample shown in Fig. 3c. So, to our luck, a less clean and thus substantially simplified vacuum procedure brings even further simplification of the technological process by eliminating a separate SiC growth step. It produces nano-

protrusions up to ~ 100 nm in height above the flat background with an areal density of $\sim 1.5 \times 10^{12} \text{ m}^{-2}$. Figs 3a and 3c are 3D renderings of the surface morphology with plotting along vertical and lateral axes not to scale. In this way, the surface features and their differences are emphasized for reader's convenience. In order to convey a true shape of protrusions, an inset in Fig. 3c shows a cross-section of a typical nanoprotusion with plotting along lateral and vertical axes performed to scale. However, even in this case, the depicted shape is not exact, due to the convolution of the shapes of the AFM probe and the surface features within the AFM image. The real nanoprotusions are certainly "sharper", meaning they are characterized by some higher aspect ratio than those seen in the inset of Fig. 3c. Because of the same circumstance, we could not exactly measure the radius of curvature at the apexes of these features, as the attempts to obtain smaller scale AFM images were only producing a more pronounced convolution of the surface features with the scanning probe shape.

3. Theoretical model

Further, we'll examine in simple approximations the emitting properties of such a structure with SiC nanoprotusions of the approximately 100-nm height on the SiC-covered silicon substrate. Unfortunately, until now there is no complete physical theory of electrons FE from semiconductor, taking into account all peculiarities of phenomenon. It is clear that emission from surface can be strongly influenced by the conditions on this surface and the type of space charge region (SCR), which can be created both by surface centers and by electric field, which can penetrate into semiconductor. Later, we shall use the realistic assumption, presented in Fig. 4: an accumulation layer with excess free electrons is formed after external field, caused by positive anode potential, is applied.

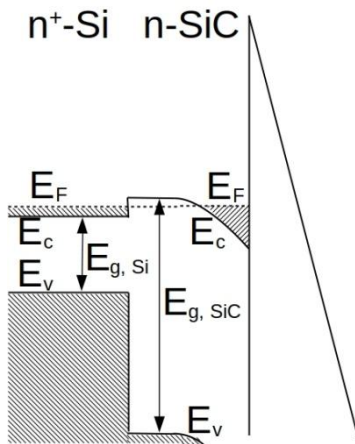


Fig. 4. Accumulation layer near the n^+ -Si/n-SiC surface with a barrier for electron tunneling in the presence of external electric field. The barrier shape neglects the image force.

The conduction band edge is shifted downwards from its bulk position E_c because of surface potential energy:

$$E = E_c^s = E_c - |\varphi_s|. \quad (1)$$

Note that a potential barrier on vacuum side with a height equal to electron affinity χ exists for electron near the conduction band bottom at the surface. FE current density from the surface is proportional to product of electron charge q ; electron velocity along the direction z across the surface; the probability for electron with the energy E to tunnel through the barrier, presented in Fig. 4, $T(E)$; and the Fermi-Dirac distribution function $f(E, E_F)$, integrated over wave vectors in the plane of the surface xy (see, e.g. [1]):

$$J = q \int_0^\infty \frac{dk_z}{2\pi} \frac{\hbar k_z}{m_e} T(k_z) \left[2 \int \frac{d\vec{k}}{(2\pi)^2} f(E, E_F) \right]. \quad (2)$$

Note that a factor in square brackets in (2) gives, in fact, a total number of surface electronic states in the energy range $[E, E_F]$. Later, we shall use simple parabolic approximation with isotropic electron effective mass:

$$E = E_c^s + \frac{\hbar^2}{2m_e} (\vec{k}^2 + k_z^2). \quad (3)$$

In this approximation, integration of the factor in square brackets in (2) yields:

$$J = \frac{q}{h} \int_0^\infty \frac{dk_z}{2\pi} \frac{\hbar k_z}{m_e} T(k_z) N_{2D} \left(E_F - E_c^s - \frac{\hbar^2 k_z^2}{2m_e} \right). \quad (4)$$

Eq. (4) includes the 2D density of states

$$N_{2D} = \frac{m_e}{\pi \hbar^2}. \quad (5)$$

After introduction of the new energy variable

$$E' = E_c^s + \frac{\hbar^2 k_z^2}{2m_e}, \quad (6)$$

for the case of strongly degenerated carriers in accumulation region near the SiC surface (as it is presented in Fig. 4), we get

$$J = \frac{q}{h} \frac{m_e}{\pi \hbar^2} \int_{E_c^s}^{E_F} T(E') (E_F - E') dE'. \quad (7)$$

Taking standard Fowler-Nordheim form for $T(E)$ in the case of tunneling through the triangular barrier, presented in Fig. 4, we finally get:

$$J = \frac{q}{2h} \frac{m_e}{\pi \hbar^2} (E_F - E_c^s)^2 \exp \left[-\frac{4\sqrt{2m} \chi^{3/2}}{3\hbar q F} \right]. \quad (8)$$

Here, F is the external electric field between emitter and anode, m – free electron mass (electron tunneling occurs into the vacuum). Note that for the case of accumulation layer presented in Fig. 4 the energy difference in pre-factor of (8) can be expressed through F .

On the one hand, the surface charge density σ can be expressed through Gauss theorem:

$$\sigma = \varepsilon_0 F_s. \quad (9)$$

Here, ε_0 is the vacuum permittivity in SI units, F_s – electric field near the surface in semiconductor with the permittivity ε_s (9.7 for SiC), which in the simplest approximation can be written as

$$F_s = F\varepsilon_s. \quad (10)$$

On the other hand, for the case presented in Fig. 2 σ can be written directly as a factor of q , 2D density of states (5), and the energy interval ($E_F - E_c^s$):

$$\sigma = q \frac{m_e}{\pi \hbar^2} (E_F - E_c^s). \quad (11)$$

With allowance for Eqs (9)–(11), Eq. (8) can be finally rewritten as:

$$J = \frac{\hbar}{4qm_e} \left(\frac{\varepsilon_0}{\varepsilon_s} \right)^2 F^2 \exp \left[-\frac{4\sqrt{2m} \chi^{3/2}}{3\hbar q F} \right]. \quad (12)$$

This expression presents formally the same dependence of the FE current density on the electric field F , as a well known expression for metals [1]:

$$J = AF^2 \exp \left[-\frac{B}{F} \right]. \quad (13)$$

Note, however, that Fowler–Nordheim formula (13) is universal for all metals. On the contrary, for semiconductors (12) describes a special case of accumulation layer near n -doped material surface (see Fig. 2). An expression for, *e.g.*, the case with high electron charge accumulated in surface traps would be different. Semiconductors, unlikely to metals, can demonstrate a variety of situations that can not be described by one unified formula.

Eq. (10) was obtained for a flat SiC surface. Now, we'll approximate the protrusions, observed experimentally, with nanocones, characterized by the average height h , diameter of the basement R , and diameter of the apex r , similar to the case of carbon nanostructures [9].

Later, we'll consider a case of comparatively low concentration of nanoprotusions, non-overlapping between each other, namely $N = 1.5 \times 10^{12} \text{ m}^{-2}$,

$$2R < 1\sqrt{N}. \quad (14)$$

Advanced examination from the surface, presented in Fig. 5, needs a numerical solution of a complicated self-consistent problem for electric field, surface potential and surface charge density in semiconductor.

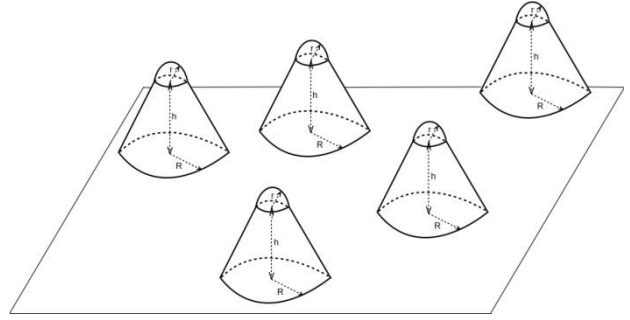


Fig. 5. A sketch of morphology of the SiC/Si(001) emitter surface with nanoprotusions. R is the average radius of the nanoprotusion basement, r is the average radius of their apex curvature, h is the average height of the nanoprotusions.

However, in zero-order approximation the emission current would be determined by the two addends: the current from the flat “bottom” and the current from the apex (in geometry, presented in Fig. 5, almost all emission from the nanoprotusion occurs through its apex, because the electric field \vec{F} component, normal to its side surface, is lower (see, *e.g.* [10]).

$$I = \frac{\hbar}{4qm_e} \left(\frac{\varepsilon_0}{\varepsilon_s} \right)^2 F^2 \exp \left[-\frac{4\sqrt{2m} \chi^{3/2}}{3\hbar q F} \right] L^2 (1 - N\pi R^2) + \frac{\hbar}{4qm_e} \left(\frac{\varepsilon_0}{\varepsilon_s} \right)^2 \beta^2 F^2 \exp \left[-\frac{4\sqrt{2m} \chi^{3/2}}{3\hbar q \beta F} \right] L^2 N\pi r^2. \quad (15)$$

The enhancement factor β can be roughly estimated for the system presented in Fig. 5 (see [10]), as:

$$\beta \approx \frac{h}{r}. \quad (16)$$

From Fig. 3c, h can be taken as $\sim 80 \text{ nm}$, $R \sim 100 \text{ nm}$, while r could not be extracted from our measurements. In principle, the self-assembly driven by electric field as in Fig. 3c can produce even atomically sharp tips. However, these can obviously be extremely unstable both while manufacturing and operation, so we take a somewhat conservative estimate for r starting from 1 nm. Fig. 6 gives the current from the Si/SiC emitter ($L = 1 \text{ m}$), calculated as a function of electric field F , for three different values of r (1, 3 and 5 nm). This gives β values of 80, 26.6 and 16. As exemplified by the 4H-SiC polytype, its electron affinity can vary substantially depending on the chemical termination of the surface [11]. Since there is no precise control of the surface termination in our experimental conditions, we adopt a blind estimate of 3 eV for the electron affinity χ . Also, as reviewed in [12], we utilize $m_e = (m^2 m_{||})^{1/3}$, $m = 0.42m_0$, $m_{||} = 0.29m_0$ for the value of the electron effective mass.

In the best case (the smallest tip radius), one can observe a turn-on electric field of $\sim 4.5 \times 10^7 \text{ V/m}$, at which the emission current of $\sim 1 \text{ mA}$ can be harvested from one square centimeter of the cathode surface.

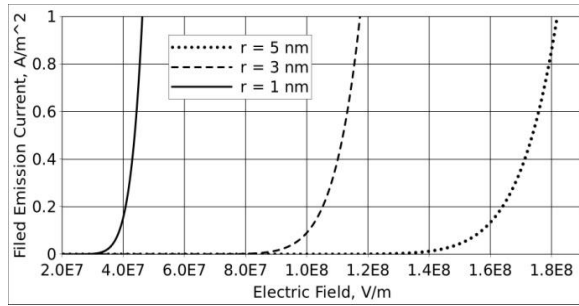


Fig. 6. Field emission current density from the Si/SiC emitter, calculated from (15) as a function of electric field F for different values of $\beta = 80$ ($r = 1$ nm), 26.6 ($r = 3$ nm), 16 ($r = 5$ nm).

It is worth noting that the values of β can reach as high as several thousands, as reported in [10]. If our self-assembly process can be tuned to produce the needles of corresponding morphology yielding such high field enhancement factors, then even lower turn-on fields can be expected. The turn-on electric field for the system under examination is essentially lower than for, e.g., the electron emission Si-based resonant-tunneling diode, examined in [13] ($\sim 2 \times 10^9$ V/m), and the relevant emission current is higher. Our results for electric field and emission current are comparable to those reviewed in [1] for GaN-based cathodes or reported for zinc oxide based cathodes [14].

4. Conclusions

In conclusion, we outline that the technological procedure of growing SiC tips on the Si substrate described in this work is substantially simpler and produces better surface morphology than the catalyst-tuned pyrolysis of polycarbosilane reported by Guo *et al.* [15]. It is also worth noting that our observations stand in line with the results of atomistic modeling of the process of electric field stimulated growth of nanotips on tungsten surfaces [16]. Possible practical applications of the Si-based self-assembled SiC nanotip emitters may take place in various novel active vacuum electron devices including those for THz frequency range and those aimed to be integrated into existing microelectronic technology, photon-gated electron emitters for generation of ultra-short electron bunches, flat panel displays, *etc.*

We have demonstrated the Si/SiC material system as a promising choice for field emission cathodes. Its main advantage is an extremely simple and cost-effective manufacturing process based on the standard microelectronics-grade silicon wafers. It integrates within a simple step both the SiC growth and the surface nanostructuring in the form of nanosized needles, which is obviously beneficial for cathode applications. A simple theoretical model, with three-dimensional geometry being neglected, predicts FE current densities and turn-on electric fields comparable to those of electron emitters based on other wide band gap semiconductors. Thus, practical device applications should be allowed.

This work was supported by the National Taras Shevchenko University of Kyiv and the Ministry of Education and Science of Ukraine (Grant № 21БП052-02).

References

1. Evtukh A., Hartnagel H., Yilmazoglu O., Mimura H. and Pavlidis D. *Vacuum Nanoelectronic Devices: Novel Electron Sources and Applications*. John Wiley & Sons, Ltd., 2015.
2. https://www.tf.uni-kiel.de/matwis/amat/semi_en/kap_a/illustr/ia_1_2.html
3. Taki Y., Kitiwan M., Katsui H., Goto T. Electrical and thermal properties of nitrogen-doped SiC. *J. Jpn. Soc. Powder and Powder Metallurgy*. 2018. **65**. P. 508–512. <https://doi.org/10.2497/jjspm.65.508>.
4. Liu W., Li Q., Yang X., Chen X. and Xu X. Synthesis and characterization of N-doped SiC powder with enhanced photocatalytic and photoelectrochemical performance. *Catalysts*. 2020. **10**. P. 769. <https://doi.org/10.3390/catal10070769>.
5. Gill V., Guduru P.R., Sheldon B.W. Electric field induced surface diffusion and micro/nano-scale island growth. *Intern. Journal of Solids and Structures*. 2008. **45**. P. 943–958. <https://doi.org/10.1016/j.ijsolstr.2007.09.010>.
6. Goryachko A., Yeromenko Y., Henkel K., Wollweber J., Schmeißer D. The Si(001)/C₂H₂ interaction to form a buffer layer for 3C-SiC growth. *physica status solidi (a)*. 2004. **201**. P. 245–248. <https://doi.org/10.1002/pssa.200303914>.
7. Goriachko A., Melnik P.V., Nakhodkin M.G. A suggestion of the graphene/Ge(111) structure based on ultra-high vacuum scanning tunneling microscopy investigation. *Ukr. J. Phys.* 2016. **61**. P. 75–87. <https://doi.org/10.15407/ujpe61.01.0075>.
8. Goriachko A.M., Kulyk S.P., Melnik P.V., Nakhodkin M.G. Scanning tunneling microscopy investigation of the Si(001)-c(8×8). *Ukr. J. Phys.* 2015. **60**. P. 148–152. <https://doi.org/10.15407/ujpe60.02.0148>.
9. Giubileo F., Di Bartolomeo A., Iemmo L., Luongo G. and Urban F. Field emission from carbon nanostructures. *Appl. Sci.* 2018. **8**. P. 526. <https://doi.org/10.3390/app8040526>.
10. Biswas D. A universal formula for the field enhancement factor. *Physics of Plasmas*. 2018. **25**. P. 043113.
11. Beattie J.M.A., Goss J.P., Rayson M.J. and Briddon P.R. Structure and electron affinity of the 4H-SiC (0001) surfaces: a methodological approach for polar systems. *J. Phys.: Condens. Matter*. 2021. **33**. P. 165003. <https://doi.org/10.1088/1361-648x/abf0be>.
12. Latreche A. Determination of temperature dependence of electron effective mass in 4H-SiC from reverse current-voltage characteristics of 4H-SiC Schottky barrier diodes. *SPQEO*. 2020. **23**. P. 271–275. <http://dx.doi.org/10.15407/spqeo23.03.271>.

13. Evtukh A., Litovchenko V., Goncharuk N., and Mimura H. Electron emission Si-based resonant-tunneling diode. *Journal of Vacuum Science and Technology B*. 2012. **30**. P. 022207. <https://doi.org/10.1116/1.3693977>.
14. Dantas M.O.S., Criado D., A. Zúñiga *et al.* ZnO nanowire-based field emission devices through a microelectronic compatible route. *Journal of Integrated Circuits and Systems*. 2020. **15**. P. 1–6. <https://doi.org/10.29292/jics>.
15. Guo C., Cheng L., Ye F., Zhang Q. Adjusting the morphology and properties of SiC nanowires by catalyst control. *Materials*. 2020. **13**. P. 5179. <https://doi.org/10.3390/ma13225179>.
16. Jansson V., Baibuz E., Kyritsakis A. *et al.* Growth fields mechanism for nanotips in high electric fields. *Nanotechnology*. 2020. **31**. P. 355301. <https://doi.org/10.1088/1361-6528/2FAB9327>.

Authors and CV



Goriachko A.M. Doctor of Sciences in Physics and Mathematics, Associate Professor of the Faculty of Radiophysics, Electronics and Computer Systems at the National Taras Shevchenko University of Kyiv. He is the author of more than 70 scientific publications. His research interests

include physics of nanostructured surfaces and 2D materials, scanning probe microscopy, electron spectroscopy and diffraction. <https://orcid.org/0000-0003-2963-5010>



Strikha M.V. Doctor of Sciences in Physics and Mathematics, Professor of the Faculty of Radiophysics, Electronics and Computer Systems at the National Taras Shevchenko University of Kyiv, Chief Researcher of the Department of Theoretical Physics at the V. Lashkaryov Institute of Semiconductor Physics, NAS of Ukraine.

He is the author of more than 200 scientific publications. His research interests include physics of 2D materials and systems, non-linear phenomena in graphene and dichalcogenides of transition metals in single layers on dielectric and ferroelectric substrates. <https://orcid.org/0000-0002-2380-0305>

Наноструктурований SiC як перспективний матеріал для холодної емісії електронів

А.М. Горячко, М.В. Стріха

Анотація. У цій роботі запропоновано нові холодні польові електронні емітери на основі наноструктурованих шарів SiC на підкладці Si(001). Їхньою головною перевагою є надзвичайно простий і низьковитратний процес виготовлення на стандартних кремнієвих пластинах, що використовуються у мікроелектроніці. Він поєднує в одному простому кроці як вирощування SiC, так і наноструктурування поверхні у формі нанорозмірних голок, які є надзвичайно вигідними з погляду застосування у катодах. При цьому не потрібно ні надвисокого вакууму, ні складного процесу хімічного осаджування з використанням токсичних хімічних речовин. Проста математична модель передбачає густини струмів емісії та порогові значення електричних полів, які дозволяють практичне застосування таких пристроїв. Згідно з нашими оцінками, для порогового поля порядку 4.5×10^7 В/м можуть бути отримані емісійні струми з поверхні катода порядку міліамперів на квадратний сантиметр. Таким чином, наноструктурований SiC може бути перспективним матеріалом для холодних електронних емітерів.

Ключові слова: холодні електронні емітери, наноструктуровані шари SiC, густина струму.